BOREAL ENVIRONMENT RESEARCH 13: 103–112
ISSN 1239-6095 (print) ISSN 1797-2469 (online)

Helsinki 28 April 2008

# Aerosol components and types in the Baltic Sea region

Aivo Reinart*, Ülle Kikas and Eduard Tamm

*Institute of Environmental Physics, University of Tartu, Ülikooli 18, 50090 Tartu, Estonia (*e-mail: aivo.reinart@ut.ee)*

*Received 20 Nov. 2006, accepted 20 Dec. 2007 (Editor in charge of this article: Veli-Matti Kerminen)*

Reinart, A., Kikas, Ü. & Tamm, E. 2008: Aerosol components and types in the Baltic Sea region. *Boreal Env. Res.* 13: 103–112.

Atmospheric aerosol observed in Estonia in summer 2002 was classified with different methods. The aim of the investigation was to identify and characterise the main aerosol types and components in order to facilitate modelling of the regional aerosol. The classification scheme used enabled to identify aerosol types proceeding from the optical characteristics of aerosol in the UV region. The optical and size distribution characteristics were specified for the following aerosol types: marine clean mixed with continental clean, marine polluted mixed with continental average, continental polluted, and continental polluted mixed with smoke. Another classification method was based on the decomposition of the measured aerosol size distributions to basic aerosol components. It enabled a flexible linking of aerosol size distribution, composition, and optical properties. Percentages (mean ± SD for 17 days) of the basic components in the aerosol volume was estimated as follows: soot = 1.2% ± 1.4%, insoluble = 23.1% ± 8.3%, water-soluble = 44.0% ± 10.8%, accumulation mode sea salt = 31.6% ± 6.2%.

## Introduction

Atmospheric aerosols may strongly affect the solar radiation reaching the Earth's surface in absence of clouds. In extreme cases, the aerosol effect may exceed the cloud effect. Decrease in the surface solar irradiance by up to 75% has been observed in the regions heavily loaded with the aerosol from biomass fires (Tarasova *et al.* 2000). Atmospheric aerosol complicates the correct prediction of photo-biologically effective exposures that are vital for natural ecosystems and health care. A short-term variability of aerosol optical depth (AOD) may induce variations in the surface UV irradiances comparable with the changes caused by the stratospheric ozone variations of 40–80 DU (Reuder and Schwander 1999). Although the satellite data have greatly improved the knowledge about atmospheric aerosols, high uncertainties of the direct aerosol effect still exist due to high spatial and temporal variation of aerosol optical properties and composition (Myhre *et al.* 2005)

The radiative effect of aerosol depends on spectral optical properties of aerosol. The critical characteristics for modelling of aerosol optical properties are the aerosol size distribution, complex refractive index, hygroscopic growth factor, particle shape, mixing type, and vertical profile (d'Almeida *et al.* 1991, Hess *et al.* 1998, Koepke *et al.* 1998). Characterisation of aerosols in the radiative transfer algorithms and climate models is a sophisticated task because of a high number of the required aerosol parameters, and the high variability of those parameters. The variability can be reduced in models by introducing

the aerosol types or components with the predefined microphysical and optical characteristics. A component-based aerosol model is widely used as a parametrisation tool in radiative transfer algorithms, e.g. for calculation of the TOMS and ENVISAT aerosol products. As an example, a Synergetic Aerosol Retrieval (SYNAER) method (Holzer-Popp *et al*. 2002) can deliver the boundary layer AOD and aerosol type both over land and over ocean. The AODs are derived for 40 boundary layer aerosol mixtures of six representative aerosol components. Introducing of components is necessary, since the retrieved values depend strongly on the aerosol microphysical properties. The methodology selects the most plausible type of aerosols from the remote sensing observations in each pixel, whereas the type selection is a mathematically ambiguous solution. This method is adapted to ENVISAT SCIAMACHY and AATSR, and is also applicable to METOP GOME-2 and AVHRR (Holzer-Popp *et al*. 2004). The major aerosol types — stratospheric, volcanic, continental, maritime, urban, desert dust, biomass burning, etc. — have been defined on the basis of long-term investigations. However, the classification schemes and the type characteristics vary by models and by geographic regions (Smirnov *et al*. 2003, Penner *et al*. 2001, Torres *et al*. 1998). Better knowledge on regional aerosol types is required for validation of satellite-based aerosol products, and improved prediction of aerosol impact on solar radiation transfer in different seasons and locations.

This article deals with the characterisation and classification of aerosol over Estonia in summer 2002, when a dramatic variation in atmospheric turbidity was observed in cloudless days. The investigation was based on the *in situ* measurements of aerosol and UV radiation, and the remote sensing data provided by the AERONET and TOMS systems (http://aeronet.gsfc.nasa.gov/, http://toms.gsfc.nasa.gov/).

The classification of aerosols according to the different schemes is described. The first one proceeded from the comparison of the AERONET AODs with the TOMS aerosol index (Torres *et al*. 1998), and enabled assessment of the optical and size distribution characteristics of different aerosol types. Another method presumed aerosol to consist of a limited number of basic aerosol components (Hess *et al*. 1998, Shettle and Fenn 1979), and enabled the apportionment of those components in aerosol.

## Methodology

### Approach

The investigation was conformed to a classification scheme (Hess *et al*. 1998) that relates aerosol types to principal aerosol emission sources and pollution level in a source area. The aerosol types like maritime clean, continental polluted or urban average can be specified in this classification. The aerosol types, in turn, are composed of a mixture of basic aerosol components with known microphysical and chemical properties. Each component combines an ensemble of particles, which are similar in their optical characteristics. Each component represents aerosols of a certain origin (soot, sea salt, desert dust, water soluble, etc.), and is an internal mixture of all chemical substances of the similar origin (Shettle and Fenn 1979). The components may be externally mixed. The used approach enabled to specify the aerosol types occurring during the measurement period, and to apportion the basic aerosol components in the *in situ* measured aerosol.

Identifying of the aerosol types started with the comparison of the TOMS aerosol index (AI) and the AODs measured by the AERONET sun photometer. The AI is a TOMS product, characterising the aerosol burden in the atmosphere. The TOMS aerosol index is a dimensionless measure of the change in the spectral contrast in the near UV spectral region due to the aerosol effect (Torres *et al*. 1998). For the absorbing aerosols, the AI is approximately proportional to the aerosol optical depth, but also depends on single scattering albedo and the height of the aerosol layer. The aerosol optical depth $\tau_a$ can be calculated from the aerosol index as follows: $\tau_a = C \times \mathrm{AI}$, whereas the proportionality factor $C$ should vary with the aerosol type (Herman *et al*. 1999). The values of $C$ evaluated from the TOMS and AERONET data were therefore used for the initial grouping of aerosol. Subsequently,

other characteristics of groups were compared, and difference of groups was tested with the statistical analysis of variance. Additionally, the back trajectory analysis was performed for association of the groups with aerosol types.

Another method was used for the apportionment of the basic aerosol components in the measured surface aerosol. The *in situ* measured aerosol volume distributions were decomposed to a set of log-normal distributions, each of which represented a basic aerosol component in real atmospheric conditions (D'Almeida *et al*. 1991, Holzer-Popp *et al*. 2004). Mathematically, such decomposition is an incorrect procedure, resulting in a non-unique solution. The ambiguity of the solution may be reduced by defining initially the number of components and by setting the external constraints about the aerosol. The decomposition results were verified with the surface UV measurements, whereas the calculations of aerosol optical properties with the OPAC code (Hess *et al*. 1998), and the radiative transfer calculations with the LibRadtran model (Mayer and Kylling 2005) had been included. A detailed description of the methodology was published in Reinart *et al*. 2006.

### Data

Measurements of UV radiation and aerosol were carried out in Pärnu, Estonia (58.38°N, 24.51°E) in July–September 2002. The aerosol size distributions were measured with the electric aerosol spectrometer EAS of the University of Tartu (Tammet *et al*. 2002). The instrument measures the electric mobility-equivalent size distribution of the aerosol in 12 size fractions, equally divided in the logarithmic diameter scale. The fraction-average diameters were 13, 24, 42, 75, 130, 240, 420, 750, 1300, 2400, 4200 and 7500 nm. The averaged aerosol size distributions for ±2 hours around the respective UV measurement time were used.

The global (direct + diffuse) UV radiation spectra (for wavelenths 300–400 nm) were measured with the UV spectrometer PC2000 (Ocean Optics Inc), calibrated with the FEL-type standard light source with traceability to NIST (Veismann and Kübarsepp 2000). The columnar aerosol AODs were obtained from the closest AERONET station in Tõravere (58.27°N, 26.47°E, http://aeronet.gsfc.nasa.gov/), the averaged values around ±3 hours of the corresponding UV measurement time were used.

The origin of the synoptic air masses and the prehistory of aerosol over Pärnu and Tõravere were investigated with the 72-hour back trajectories, calculated with the HYSPLIT model (http://www.arl.noaa.gov/ready/hysplit4.html). The local meteorological data of the Pärnu harbour (http://ilm.transcom.ee/), the aerosol index, and the total ozone data from the TOMS (http://toms.gsfc.nasa.gov/) were also used.

## Results and discussion

### Variation of aerosol characteristics

In the Baltic region, the summer of 2002 was extreme in terms of high air temperatures, little precipitation, large number of cloudless days and a drought in July–August. The clear-sky surface irradiances were strongly influenced by the atmospheric aerosol. Remarkable diminishing of UV irradiances was observed in several cloudless periods (10–11 and 29–31 July; 15, 19–20 and 24–29 August). At the end of August, the aerosol haze obscured the sky and decreased the horizontal visibility. The range of AOD variation in the Baltic Sea region was the highest in the summers of 1997–2002 (Jaruslawski *et al*. 2003). The value of AOD at 340 nm ($AOD_{340}$) in Tõravere reached maximum values up to 2.2 ($AOD_{500}$ up to 1.8), and the midday UV indices in Pärnu were diminished by up to 53% as compared with those expected for the aerosol-free atmosphere (Fig. 1). The observed variations in the aerosol turbidity and the surface irradiances were obviously caused by changing aerosol properties.

The proportionality factor $C$ between the TOMS aerosol index and AERONET AOD showed varying values which presumably exhibited the alternation of aerosol types. A linear dependence between the proportionality factor $C$ and the AOD was found for the turbid atmosphere ($AOD_{340} > 0.3$) (Fig. 2). Thus, the scatterplot in Fig. 2 can be interpreted as a distribution of the aerosol types according to their radiative

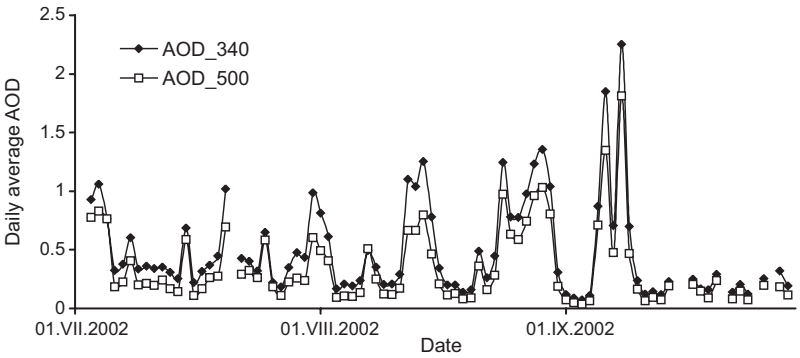


**Fig. 1**. Variation of AOD in Tõravere.

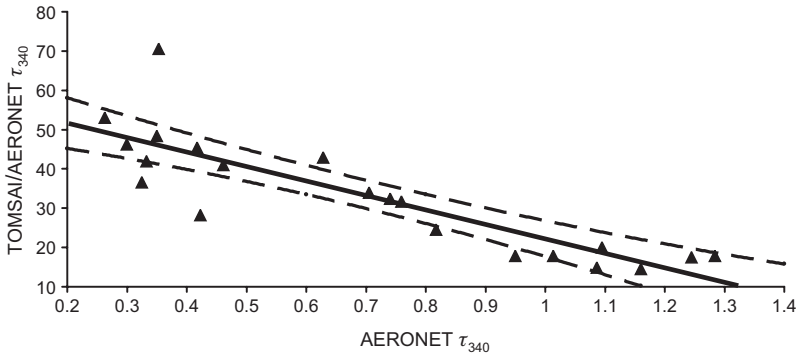


**Fig. 2**. Dependence of the proportionality factor *C* on aerosol optical depth $\tau_{340}$. The dashed lines indicate 95% confidence level.

effect in the UV region. For the clean atmosphere ($AOD_{340} < 0.3$), however, no correlation between *C* and AOD was found, while the AI showed enormous negative values. This discrepancy can be explained by the high uncertainty of the TOMS AI estimations in the clean atmosphere, affected by the surface reflectivity (Torres *et al*. 2002). Four aerosol groups were distinguished from the above-described comparison of the columnar aerosol optical characteristics. Three groups represented the AOD values shown in Fig. 2, the fourth group assembled the days with the small AOD values ($AOD_{340} < 0.2$). Each group represented four to eight cloudless days from the period July–September 2002. Although the grouping procedure was ambiguous, it enabled a least arbitrary classification of aerosol according to its optical effect. The group-mean optical and microphysical characteristics (Table 1) were obtained from the AERONET and EAS measurements, and difference between the groups was tested by the statistical analysis of variance. Further, the groups were associated with the prevailing air back trajectories, which enabled to assess the aerosol types. A continental clean/marine clean (CC/MC) aerosol type was assigned to the aerosol from the Arctic or the North Atlantic, carried over Scandinavia; a continental average/marine polluted (CA/MP) type to the aerosol from the Atlantic, transported over the northern part of Europe (British Islands, Denmark, the Baltic Sea); a continental polluted (CP) type corresponded to the back trajectories over central and eastern Europe (Germany, Poland, Ukraine, Russia); a continental polluted with smoke (CP + smoke) to the aerosol transported from the eastern and north-eastern continental areas (Russia, Russian Arctic), and polluted with the emissions from the biomass fires, registered during this period.

All four aerosol types differed from each other (at 95% confidence level) in major optical characteristics (AODs $\tau$, Ångström coefficient $\alpha$, real part of the refractive index *n*), and aerosol volume concentration ($Vol_F$ and $V_F$) in the optically active diameter range (Table 1). In general, the aerosol optical depth increased with the increasing fine aerosol number concentration $N_F$ and volume concentration $V_F$ at the surface, and in the total aerosol column ($Vol_F$). However,

a remarkable difference occurred in the aerosol effective radii ($R_{eff}$), whereas AERONET-retrieved radius was systematically smaller than the radius measured by EAS. The result may refer to the different size distributions of surface and columnar aerosol, but also to the systematic difference between the data acquisition methods.

The contradictory optical characteristics have been obtained for the CC/MC aerosol type: the low AODs occurred simultaneously with the high absorption ability ($k_{441}$) and low single scattering albedo ($ssa_{441}$). It can be explained by high uncertainties of the AERONET retrievals for clean atmosphere, claimed by the AERONET team. Another peculiarity of the CC/MC aerosol type was the highest share of ultrafine particles (diameter < 0.1 $\mu$m) and the lowest share of fine particles (0.10 $\mu$m ≤ diameter ≤ 1.2 $\mu$m). The result is consistent with the several reports about the bursts of ultrafine aerosol particles observed in the air of the Arctic and North-Atlantic origin. The bursts occur due to nucleation events in case of low background aerosol concentration (Nilsson *et al*. 2001, Vana *et al*. 2004).

Variation of the aerosol type strongly affected scattering of the incident solar radiation by aerosol, as can be seen from Fig. 3, where the scattering coefficients per unit aerosol mass for two incident wavelengths are presented. The scattering coefficients were calculated with the Mie theory for spherical particles (Bohren and Huffmann 1983). A similar comparison of the extinction coefficients was unfortunately unreliable because of the above mentioned uncertainties in the absorption coefficients.

The classification has revealed the typical properties of the regional clear sky aerosol, and their relation to the typical air mass trajectories. This method, however, is poorly applicable for online characterisation of aerosol, since the discrete aerosol types rarely occur.

## Apportionment of aerosol components

A more flexible approach for aerosol classification was tested. The method was based on decomposition of *in situ* aerosol size distributions to the standard aerosol components, and subsequent calculation of the optical properties

**Table 1**. Characteristics of the aerosol types. Numerical subscripts indicate radiation wavelengths (nm). Subscripts F and UF indicate fine (0.10 µm ≤ diameter ≤ 1.2 µm) and ultrafine particles (diameter < 0.1 µm), respectively. The EAS $R_{eff\_F}$ is calculated in accordance to AERONET formulas (Smirnov *et al.* 2000). *n* and *k* are the real and imaginary parts of the refractive index, respectively, and ssa is the single scattering albedo.

| | Aerosol type | Air trajectory | Days | AERONET | | | | | | | Electric Aerosol Spectrometer (EAS) | | | |
|---|---|---|---|---|---|---|---|---|---|---|---|---|---|---|
| | | | | $\tau_{500}$ | $\tau_{340}$ | $\alpha_{440\text{-}870}$ | $ssa_{441}$ | $n_{441}$ | $k_{441}$ | $Vol_F$ (µm³ µm⁻²) | $R_{eff\_F}$ (µm) | $N_F$ (cm⁻³) | $N_{UF}$ (cm⁻³) | $V_F$ (µm³ cm⁻³) | $R_{eff\_F}$ (µm) |
| 1 | CC/MC | N-NW | 8 | 0.07 | 0.13 | 1.19* | 0.78* | 1.36* | 0.034* | 0.01 | 0.14 | 948 | 4986 | 1.27 | 0.20 |
| 2 | CA/MP | W | 7 | 0.20 | 0.35 | 1.61 | 0.92 | 1.37 | 0.012 | 0.04 | 0.15 | 1378 | 2905 | 2.13 | 0.19 |
| 3 | CP | S-SE | 4 | 0.49 | 0.76 | 1.58 | 0.92 | 1.42 | 0.011 | 0.12 | 0.12 | 2780 | 3922 | 4.35 | 0.19 |
| 4 | CP + smoke | E-SE | 6 | 0.85 | 1.15 | 1.27 | 0.95 | 1.48 | 0.009 | 0.12 | 0.15 | 2630 | 3969 | 4.63 | 0.20 |

CC = Continental Clean, CP = Continental Polluted, CA = Continental Average, MC = Maritime Clean, MP = Maritime Polluted. * = AERONET has claimed high uncertainties for very clean atmosphere.

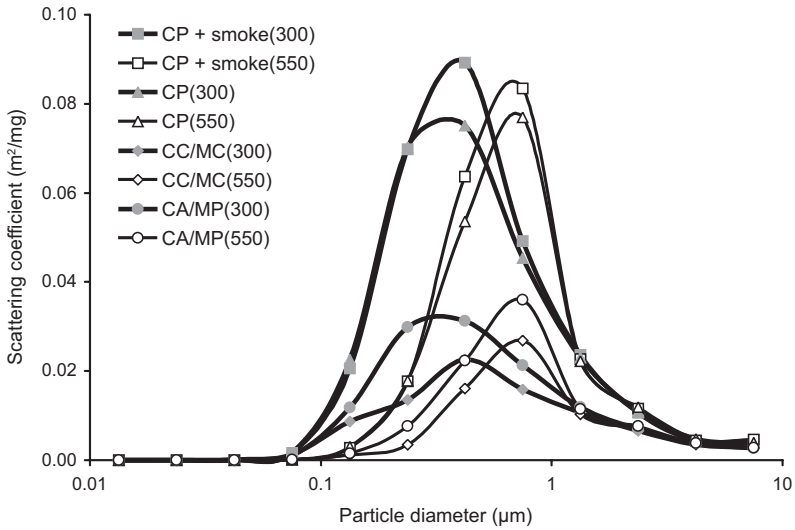


**Fig. 3**. Dependence of aerosol scattering coefficients per unit mass on aerosol diameter for different aerosol types at incident wavelengths 300 nm and 550 nm.

of component mixtures by the OPAC model. Seven aerosol components were initially considered as probable in our geographic region (Shettle and Fenn 1979, Penner *et al*. 2001, Holzer-Popp *et al*. 2002, Myhre *et al*. 2005). The component characteristics (Table 2) present the properties of the dry aerosol (for relative humidity < 40%), whereas the modal radiuses of hygroscopic components change with the ambient relative humidity. In the decomposition procedure the component parameters were modified according to the actual relative humidity with the help of look-up tables of the OPAC model (Hess *et al*. 1998). Differencing between the hygroscopic and non-hygroscopic aerosol components was one of the advantages of the component-based approach.

**Table 2**. Properties of dry aerosol components (Hess *et al*. 1998, Penner *et al*. 2001), where $r_N$, $\sigma$, $r_V$ are the parameters of lognormal size distribution: the number distribution modal radius, the geometric standard deviation, the volume distribution modal radius; $\rho$ is the particle density.

| Component | $r_N$ (μm) | $\sigma$ | $r_V$ (μm) | $\rho$ (g cm$^{-3}$) |
|---|---|---|---|---|
| Soot | 0.012 | 2 | 0.05 | 1 |
| Insoluble | 0.471 | 2.51 | 6 | 2 |
| Water-soluble | 0.021 | 2.24 | 0.15 | 1.8 |
| Sea salt (acc. mode) | 0.209 | 2.03 | 0.94 | 2.2 |
| Sea salt (coarse mode) | 1.75 | 2.03 | 7.90 | 2.2 |
| Mineral transported | 0.5 | 2.2 | 3 | 2.6 |
| Biomass regional haze | 0.08 | 1.9 | 0.26 | 1.8 |

The decomposition of *in situ* aerosol volume distributions (Fig. 4) was tested with 6, 5 and 4 components, in order to seek the most appropriate composition of components. Two concurrently good decomposition results were obtained (Table 3): a set of five components, including biomass haze, and a set of four components (with the parameters varying within ±10%). Since the method itself cannot differentiate between the two solutions, external information was used. Comparison of the two solutions showed disadvantages of the five-component model. The water-soluble and the biomass-haze components were overlapped at relative humidity of 50%–80%. In the fitting procedure those components were competing for the same aerosol volume: the percentage of the water-soluble component remarkably decreased when the biomass haze was included (Table 3). The biomass-haze content was permanently high even in beginning of July, when no biomass fires were registered. The four-component solution was therefore selected as the most relevant to the meteorological and back trajectory data. It enabled to attribute the temporal variation of the total aerosol volume during 17 days to the variation of the following components (Fig. 5): soot (1.2% ± 1.4%), insoluble (23.1% ± 8.3%), water-soluble (44.0% ± 10.8%) and accumulation mode sea salt (31.6% ± 6.2%). The apportionment showed a

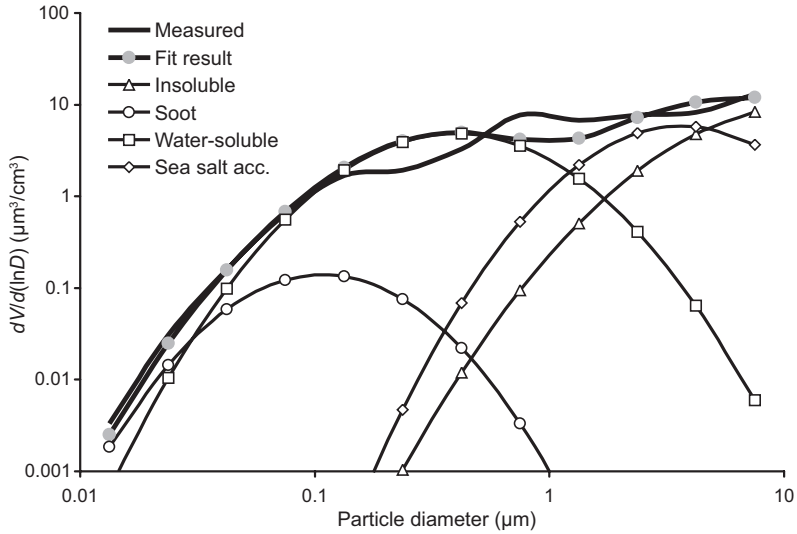


**Fig. 4**. Example of decomposition of the EAS-measured aerosol volume distribution to aerosol components defined by Hess *et al.* (1998).

high share of the hygroscopic aerosol (the water-soluble and sea-salt components) in the region. The hygroscopic aerosol is sensitive to variations in the relative humidity, and participates in the cloud formation processes.

The decomposition results were validated by comparison of the measured surface UV irradiances with the calculated ones. The calculations were performed with the UV radiative transfer code LibRadtran (Mayer and Kylling 2005) using two different aerosol entries: (1) the aerosol optical properties calculated for the mixture of decomposed aerosol components, and (2) the aerosol retrievals obtained from AERONET. Both model approaches yielded agreeable surface UV irradiances ($R^2$ = 0.91), which indirectly proofed similarity of the EAS-based and AERONET aerosol properties. However, the modelled UV irradiances were remarkably overestimated against the measurements. The difference between the measured and the modelled UV irradiances depended also on aerosol type: it was generally higher for the continental aerosol. The discrepancy between the modelled and measured UV irradiances can only partly be explained by UV measurement errors (Kikas *et al.* 2004). A part of the difference may occur because of the increased extinction of UV radiation (especially UV-B radiation) in continental aerosol, not considered in the model.

The component-based modelling of aerosol properties was successfully applied for the processing of the SeaWiFS and MODIS satellite images of the Baltic Sea (Reinart *et al.* 2004). The capability of the method can be increased by justification of the atmospheric properties of the basic components. The parameters of the lognormal components are still under scientific discussion. This work demonstrated the need for more flexible definition of component size distributions. The best results were obtained when the variation of the size distribution parameters within ±10% was tolerated.

The most disputable are the characteristics of the soot component. A small modal radius of 0.05 $\mu$m was specified according to the extinc-

**Table 3**. Average percentages of aerosol components in the measured aerosol volume distributions. Mean values and standard deviations of mean for 17 days are presented.

| | Soot | Insoluble | Water-soluble | Sea salt acc. mode | Biomass haze | Fitting error (%) | Fitted volume (%) |
|---|---|---|---|---|---|---|---|
| Variable $r_v$, $\sigma$ ± 10% | 1.2 ± 1.4 | 23.1 ± 8.3 | 44.0 ± 10.8 | 31.6 ± 6.2 | 0 | 7.6 | 98.4 |
| Fixed $r_v$, $\sigma$ + biomass haze | 1.9 ± 1.8 | 23.0 ± 10.1 | 14.2 ± 8.2 | 23.7 ± 12.8 | 36.6 ± 12.6 | 5.9 | 99.5 |

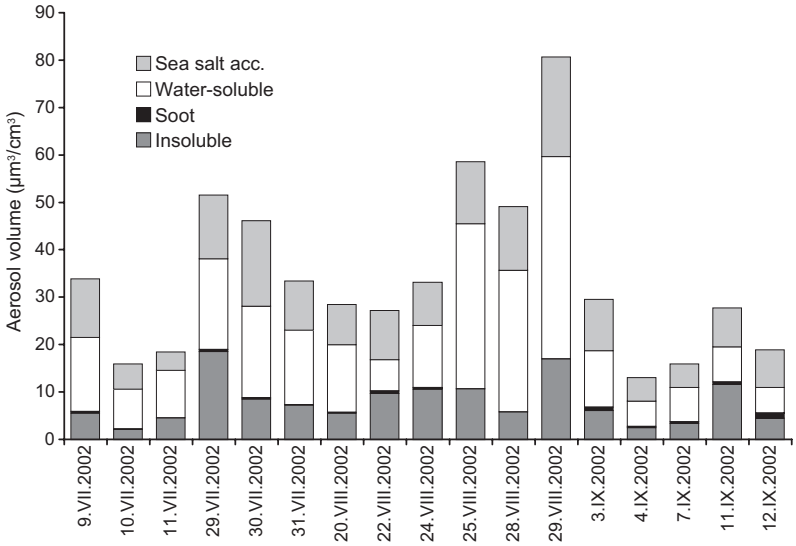


**Fig. 5**. Variation of the content of aerosol components in total aerosol volume in cloudless days.

tion properties of elementary soot particles, which, however, can aggregate during atmospheric processing. Aged soot aerosol may therefore have an optical effect, equivalent to the elementary soot particles, but the number and volume size distributions may be consistent to the aggregated soot (Schnaiter *et al*. 2003, Reinart *et al*. 2006). Recent investigations have shown also different absorption properties of diesel and biomass burning soot (Holzer-Popp *et al*. 2004). Justification of the soot component parameters requires further investigation of soot emission, transfer and aging in the atmosphere. Improvement of the knowledge on the hygroscopic growth of aerosol with changing chemical composition is also required.

## Conclusions

Atmospheric aerosols strongly decreased the surface solar irradiances in cloudless periods in summer 2002. The midday UV irradiances and daily UV exposures were diminished by up to 50% as compared with those typical for the aerosol-free atmosphere. The investigation specified the optical and microphysical characteristics of the atmospheric aerosol over Estonia in this period.

A method, based on comparison of the TOMS aerosol index and the aerosol optical depth resulted in the identification of four aerosol types: continental clean/marine clean (CC/MC); continental average/marine polluted (CA/MP); continental polluted (CP), and continental polluted including smoke (CP + smoke). Each type represented the air back trajectories over certain geographic regions, and therefore, corresponded to a specific prehistory of aerosol. The types differed in their radiative properties (aerosol optical depth, Ångström coefficient $\alpha$), but also in their microphysical properties (real part of refractive index, total aerosol volume, particle size distribution, size dependence of scattering efficiency) (Table 1). The continental aerosol types CP and CP + smoke caused higher turbidity of the atmosphere, and a higher (relative) decrease in the surface UV irradiances. The obtained typical aerosol characteristics would be helpful for modelling the aerosol radiative effects in the region.

The component composition of aerosol was also investigated. The decomposition of the measured aerosol size distributions resulted in the average apportionment of the basic aerosol components as follows: soot (1.2% ± 1.4%), insoluble (23.1% ± 8.3%), water-soluble (44.0% ± 10.8%) and accumulation-mode sea salt (31.6% ± 6.2%) of the total aerosol volume. The refractive index (for the wavelength of 440 nm) calculated for the component mixture was $1.42 - 0.013i$, which is close to the refractive index of $1.38 - 0.019i$

obtained from the AERONET retrievals. While the decomposition method provides a flexible way for modelling the aerosol optical properties from the *in situ* size distribution measurements, it has disadvantages because of the ambiguity of the mathematical solution.

Classification of aerosol with the independent methods enabled to assess the characteristics of aerosol types, and reduce the aerosol variability to the variation of basic aerosol components with the known characteristics. Matching of the obtained types and components, unfortunately, failed due to insufficient data for statistical linking.

*Acknowledgements*: This work was partly supported by the grants ETF5387 and ETF6988. The authors wish to thank M. Vaht, H. Iher, U. Veismann, T. Bernotas, A. Mirme, A. Kallis and J. Tenson for the help with measurements and calibration. The authors give their thanks to O. Kärner and M. Sulev for maintaining the AERONET station in Tõravere.

## References

Bohren C.F. & Huffman D.R. 1983. *Absorption and scattering of light by small particles*. Wiley, New York.

D'Almeida G.A., Koepke P. & Shettle E.P. 1991. *Atmospheric aerosols, global climatology and radiative characteristics*. Deepack, Hampton, Va.

Dubovik O., Holben B.N., Eck T.F., Smirnov A., Kaufman Y.J., King M.D., Tanre D. & Slutsker I. 2002. Variability of absorption and optical properties of key aerosol types observed in worldwide locations. *J. Atmos. Sci.* 59: 590–608.

Herman J.R., Krotkov N., Celarier E., Larko D. & Labow G. 1999. Distribution of UV radiation at the Earth's surface from TOMS-measured UV-backscattered radiances. *J. Geophys. Res.* 104: 12059–12076.

Hess M., Koepke P. & Schult I. 1998. Optical properties of aerosols and clouds: the software package OPAC. *Bull. Am. Meteorol. Soc.* 79: 831–844.

Holzer-Popp T., Schroedter M. & Gesell G. 2002. Retrieving aerosol optical depth and type in the boundary layer over land and ocean from simultaneous GOME spectrometer and ATSR-2 radiometer measurements. 1: Method description. *J. Geophys. Res.* 107(D24), doi:10.1029/2001JD002013.

Holzer-Popp T., Schroedter-Homscheidt M. & Kästner M. 2004. Satellite based climatology of aerosol components. In: *Proceedings of the 2004 EUMETSAT Meteorological Satellite Conference, Prague, 31.5–4.6.2004*, EUMETSAT, Germany, pp. 457–463.

Jaruslawski J., Kryscin J.W., Puchalski S. & Sobolevski P. 2003. On the optical thickness in the UV range: Analysis of the ground-based data taken at Belsk, Poland. *J. Geophys. Res.* 108(D23), 4722, doi:10.1029/2003JD003571.

Kikas Ü., Reinart A. & Sherman I. 2004. Assessment of aerosol types in the Baltic Region using TOMS and AERONET aata. In: Kasahara M. & Kulmala M. (eds), *Nucleation and Atmospheric Aerosols, 16th International Conference*, Kyoto, Japan, Kyoto University Press, pp. 682–685.

Koepke P., Bais A., Balis D., Buchwitz M., DeBacker H., de Cabo X., Eckert P., Eriksen P., Gillotay D., Heikkilä A., Koskela T., Lapeta B., Litynska Z., Lorente J., Mayer B., Renaud A., Ruggaber A., Schauberger G., Seckmeyer G., Seifert P., Schmalwieser A., Schwander H., Vanicek K. & Weber M. 1998. Comparison of models used for UV index calculations. *Photochemistry and Photobiology* 67: 657–662.

Koepke P., Hess M., Schult I. & Shettle E.P. 1997. *Global aerosol data set*. Report 243, Max-Planck-Institut für Meteorologie, Hamburg.

Mayer B. & Kylling A. 2005. The libRadtran software package for radiative transfer calculations: Description and examples of use. *Atmos. Chem. Phys.* 5: 1855–1877.

Myhre G., Stordal F., Johnsrud M., Diner D.J., Geogdzhayev I.V., Haywood J.M., Holben B., Holzer-Popp T., Ignatov A., Kahn R., Kaufman Y.J., Loeb N., Martonchik J., Mishchenko M.I., Nalli N.R., Remer L.A., Schroedter-Homscheidt M., Tanre D., Torres O. & Wang M. 2005. Intercomparison of satellite retrieved aerosol optical depth over ocean during the period September 1997 to December 2000. *Atmos. Chem. Phys.* 5: 1697–1719.

Nilsson E.D., Paatero J. & Boy M. 2001. Effects of air masses and synoptic weather on aerosol formation in the continental boundary layer. *Tellus* 53B: 462–478.

Penner J.E., Andreae M., Annegarn H., Barrie L., Feichter J., Hegg D., Jayaraman A., Leaitch R., Murphy D., Nganga J. & Pitari G. 2001. Aerosols, their direct and indirect effects. In: Houghton H.T., Ding Y., Griggs D.J., Noguer M., van der Linden P.J., Dai X., Maskell K. & Johnson C.A. (eds.), *Climate change 2001: The scientific basis*, Report to Intergovernmental Panel on Climate Change from the Scientific Assessment Working Group (WGI), Cambridge University Press, pp. 289–416.

Reinart A.E., Reinart A.T. & Kikas Ü. 2004. Estimation of aerosol optical properties used in the atmospheric correction of SeaWiFS images over Baltic Sea. In: *Abstracts of the European Aerosol Conference 2004*, Budapest, Hungary, Elsevier, pp. 537–538.

Reinart A., Kikas Ü. & Tamm E. 2006. Investigation of aerosol components influencing atmospheric transfer of UV radiation in Baltic Sea region. *J. Geophys. Res.* 111, doi:10.1029/2005JD005786.

Reuder J. & Schwander H. 1999. Aerosol effects on UV radiation in nonurban regions. *J. Geophys. Res.* 104: 4065–4067.

Shettle E.P. & Fenn R.W. 1979. *Models of aerosols of lower troposphere and the effect of humidity variations on their optical properties*. AFCRL Tech. Rep. 79 0214, Air Force Cambridge Research Laboratories, Hanscom Air Force Base, Mass.

Smirnov A., Holben B.N., Eck T.F., Dubovik O. & Slutsker I. 2000. Cloud screening and quality control algorithms for the AERONET database. *Rem. Sens. Env.* 73: 337-349.

Smirnov A., Holben B.N., Dubovik O., Frouin R., Eck T.F. & Slutsker I. 2003. Maritime component in aerosol optical models derived from Aerosol Robotic Network data. *J. Geophys. Res.* 108(D1), 4033, doi:10.1029/2002JD002701.

Tammet H., Mirme A. & Tamm E. 2002. Electrical aerosol spectrometer of Tartu University. *Atmos. Res.* 62: 315–324.

Tarasova T., Nobre C.A., Eck T.F. & Holben B.N. 2000. Modelling of gaseous, aerosol and cloudiness effects on surface solar irradiance measured in Brazil's Amazonia 1992–1995. *J. Geophys. Res.* 105: 26961–26969.

Torres O., Bhartia P.K., Herman J.R., Ahmad Z. & Gleason J. 1998. Derivation of aerosol properties from satellite measurements of backscattered ultraviolet radiation: Theoretical basis. *J. Geophys. Res.* 103: 17099–17110.

Torres O., Bhartia P.K., Herman J.R., Sinyuk A., Ginoux P. & Holben B. 2002. A long-term record of aerosol optical depth from TOMS observations and comparison to AERONET measurements. *J. Atmos. Sci.* 59: 398–413.

Vana M., Kulmala M., Dal Maso M., Hõrrak U. & Tamm E. 2004. Comparative study of nucleation mode aerosol particles and intermediate air ions formation event at three sites. *J. Geophys. Res.* 109, D17201, doi: 10.1029/2003JD004413.

Veismann U. & Kübarsepp T. 2000. Stability monitoring of radiometric standard lamp using solar blind phototube. In: *Proceedings of the 7th Biennial Baltic Electronic Conference (BEC'2000)*, Tallinn University of Technology, Tallinn, pp. 281–284.